MECSOL 2022 - Proceedings of the 8th International Symposium on Solid Mechanics
M.L. Bittencourt, J. Labaki, L.C.M. Vieira Jr. and E. Mesquita (Editors), Campinas SP, Brazil, October 17th to 19th, 2022

Wave Propagation and Band Structure Manipulation with Fractal Phononic Crystals

Victor Gustavo Ramos Costa Dos Santos[1,2], Edson Jansen Pedrosa de Miranda Jr.[1,3,4] and José Maria Campos Dos Santos[1]

[1] University of Campinas, UNICAMP-FEM-DMC, Rua Mendeleyev, 200, CEP 13083-970, Campinas, SP, Brasil
[2] Federal Institute of São Paulo, IFSP-CFM, Avenida Thereza Ana Cecon Breda, 1896, CEP 13183-250, Hortolândia, SP, Brasil
[3] Federal Institute of Maranhão, IFMA-PPGEM, Avenida Getúlio Vargas, 4, CEP 65030-005, São Luís, MA, Brasil
[4] Federal Institute of Maranhão, IFMA-EIB-DE, Avenida Afonso Pena, 174, CEP 65010-030, São Luís, MA, Brasil

The possibilities of influencing the behavior of propagating waves using the appropriate choice of materials is a field of interest in engineering. Traditional materials have very limited control of sound waves. Thus, new artificial composite materials with good vibration absorbing properties are needed to solve this problem. This paper presents the study for a two-dimensional (2-D) Sierpinski and Quasi-Sierpinski fractal phononic crystals (PnC). These PnC consist of various lattice inclusions of two materials with large impedance mismatch in a rubber matrix. The inclusions present square and circular cross sections and are concentrically aligned. The chosen materials allow elastic waves to be forbidden from propagation within certain frequency bands, the so-called band gaps or stop bands. Structures with fractal distributions and higher stages favor the appearance of several absolute gaps and with larger bandwidth. The band structure and wave mode shapes are calculated by the Finite Element (FE) and Plane Wave Expansion (PWE) methods, considering the Bloch-Floquet boundary conditions applied to all sides of the unit cell to form the periodic structure.
Keywords: Phononic crystals, Sierpinski carpet fractal, band gap

INTRODUCTION

The study of wave propagation in heterogeneous elastic and acoustic media has gained more and more notoriety in recent years, mainly due to the growing popularity of products and construction techniques that appeal to acoustic comfort, such as minimizing impacts generated by noise, and also in reducing external vibrations in sensitive buildings (Gupta, 2014; Spiousas et al., 2015). Phononic crystals (PnC) are examples of structures studied to control and reduce the propagation of these types of mechanical waves. Usually they are defined as artificial materials composed of a periodic assembly of two or more materials with large impedance mismatch (Arjunan, Baroutaji and Robinson, 2022). Thus, depending on the PnC periodicity, there are frequency bands in which waves are forbidden, giving rise to forbidden zones, or Bragg-type band gaps, which come from an analogous concept for electromagnetic waves. These new materials become interesting due to the physics applied to the modeling of mechanical systems, where the waves can have transverse and longitudinal propagation modes. Unlike band gaps formed by Bragg scattering, local resonance does not directly depend on the symmetric and periodic properties of PnC. Combining PnC with the application of locally resonant inclusions give rise to locally resonant phononic crystals (LRPnC). These are usually composed of compliant polymer (with a stiffness five orders lower than common materials) and other stiffer material in order to get low frequency gaps, which can lead to promising applications such as vibration attenuation in low frequencies or soundproofing. Recently, Miranda Jr. et al. (2019) evaluated the application of local resonators in meta-concrete structures. Sellami et al. (2019) presented a new combination of materials to define LRPnC, being a heavy core (carbon) coated by a first layer of polymer (silicone rubber) and then a second layer of carbon. From the band structures, several narrow band gaps were found, indicating that they have potential applications for acoustic noise filtering in phononic metamaterials. In both works, these structures were modeled and analyzed by the Plane Wave Expansion (PWE) method or variations of this method. Figure 1 shows some possible configurations of LRPnC unit cells.

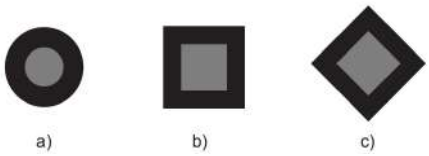

Figure 1 – Configurations of LRPnC unit cells: a) circular; b) square; and c) rotated square with a 45º angle. (Adapted from Miranda Jr et al., 2019).

This work evaluates the flexural waves through a crystal isotropic Kirchhoff-Love thin plate made of a two-dimensional (2D) array of structural units that exhibit localized resonances. It will be shown that the resonant characteristics in the band structure can be described by locally resonant band gaps and flat bands. LRPnCs are identified as ternary systems, consisting of an epoxy matrix with steel cylinders coated with silicone "rings". The existence of gaps in a frequency range two orders of magnitude lower than the resulting Bragg scattering mechanism is observed and the origin of this phenomenon is due to localized resonances associated with the scattering mechanism.

1 MATHEMATICAL FORMULATION

1.1 Plane Wave Expansion

The band structure referring to the behavior of waves propagating in the phononic crystal is determined by two methods: Plane Wave Expansion - PWE and by Finite Elements - from COMSOL. Firstly, the PWE formulation for a 2D PnC thin plate (Miranda Jr. et al., 2019) is used to determine the band structure of wave propagation restricted to the plane $(x-y)$, solving the eigenvalue problem only for the First Irreducible Brillouin Zone (FIBZ). The govern differential equation is given by (Sigalas, 1992):

$$-\alpha\frac{\partial^2 w}{\partial t^2} = \frac{\partial^2}{\partial x^2}\left(D\frac{\partial^2 w}{\partial x^2}+\beta\frac{\partial^2 w}{\partial y^2}\right)+2\frac{\partial^2}{\partial x\partial y}\left(\gamma\frac{\partial^2 w}{\partial x\partial y}\right)+\frac{\partial^2}{\partial y^2}\left(D\frac{\partial^2 w}{\partial y^2}+\beta\frac{\partial^2 w}{\partial x^2}\right), \tag{1}$$

where w is the transverse displacement, $D=\frac{Eh^3}{12(1-\nu^2)}$ is the flexural rigidity with E being the Young's modulus and ν is the Poisson's ratio, $\alpha=\rho h$, $\beta=D\nu$, and $\gamma=D(1-\nu)$ are periodic functions of the position vector $\mathbf{r}(x,y)$. Applying the Floquet-Bloch's theorem, the w can be expressed as $w(\mathbf{r},t)=e^{j(\mathbf{k}\cdot\mathbf{r}-\omega t)}w_{\mathbf{k}}(r)$. With $\mathbf{k}=(k_x,k_y)$, the Bloch wave vector, ω, angular frequency, t, time, and $j=\sqrt{-1}$. $w_{\mathbf{k}}$ has periodicity equivalent to the periodicity of the phononic crystal and is expanded in Fourier series as:

$$w_{\mathbf{k}}=\sum_{\mathbf{g}_1}e^{j\mathbf{g}_1\cdot\mathbf{r}}A_{\mathbf{g}_1}, \tag{2}$$

$\mathbf{g}_1=\frac{2\pi}{a}(n_1,n_2)$ is 2D reciprocal lattice vector for square lattice with n_1 and n_2 = $[0,\pm1,\pm2,...,\pm n]$, a is the lattice parameter and the Fourier coefficient, $A_{\mathbf{g}_1}$. The periodic functions, $\alpha(\mathbf{r})$, $\beta(\mathbf{r})$, $D(\mathbf{r})$ and $\gamma(\mathbf{r})$, are expanded in Fourier series as:

$$H(\mathbf{r})=\sum_{\mathbf{g}_2}e^{j\mathbf{g}_2\cdot\mathbf{r}}H_{\mathbf{g}_2}, \tag{3}$$

$H(\mathbf{r})$ is one of the plate parameters. The corresponding Fourier coefficient is given by:

$$H_{\mathbf{g}_2}=\begin{cases} fH_A+(1-f)H_B & for \quad \mathbf{g}_2=\mathbf{0} \\ (H_A-H_B)F_{\mathbf{g}_2} & for \quad \mathbf{g}_2\neq\mathbf{0} \end{cases}, \tag{4}$$

with $\mathbf{g}_2=\frac{2\pi}{a}(\bar{n}_1,\bar{n}_2)$, $\bar{n}_1$ and $\bar{n}_2$ = $0,\pm1,\pm2,...,\pm n$, $H_{\mathbf{g}_2}$ refers to a Toeplitz matrix, f is defined as the ratio between the cross sectional area of a cylinder and primitive unit cell, i.e., filling fraction of inclusion, and the structure function, $F_{\mathbf{g}_2}$, is defined as:

$$F_{\mathbf{g}_2}=\frac{1}{S}\int_S e^{-j\mathbf{g}\cdot\mathbf{r}}dr^2, \tag{5}$$

where S refers to the area of the unit cell and the integral operator being calculated over the cross section of the host material.

1. In cases where the PnC consists of circular cylinder inclusions (radius r_o), the filling fraction is given by:

$$f = \frac{\pi r_o^2}{a^2} \quad \text{and} \quad F_{\mathbf{g}_2} = \frac{2f}{|\mathbf{g}_2| r_o} J_1(|\mathbf{g}_2| r_o), \tag{6}$$

   where $J_1(|\mathbf{g}_2| r_o)$ is the Bessel function of the first kind.

2. For square section of width $2l$

$$f = \frac{4l^2}{a^2} \quad \text{and} \quad F_{\mathbf{g}_2} = f \frac{\sin(g_1 l)}{(g_1 l)} \frac{\sin(g_2 l)}{(g_2 l)}. \tag{7}$$

Substituting the considerations of displacement fields of flexural waves and the Eq. (3) in Eq. (1), we can express the following eigenvalue problem:

$$\begin{aligned} \omega^2 \sum_{\mathbf{g}_1} [\alpha]_{\mathbf{g}_2} A_{\mathbf{k}+\mathbf{g}_1} &= \sum_{\mathbf{g}_1} (\mathbf{k}+\mathbf{g}_1)_x^2 (\mathbf{k}+\mathbf{g}_3)_x^2 [D]_{\mathbf{g}_2} A_{\mathbf{k}+\mathbf{g}_1} + \\ &+ \sum_{\mathbf{g}_1} (\mathbf{k}+\mathbf{g}_1)_y^2 (\mathbf{k}+\mathbf{g}_3)_x^2 [\beta]_{\mathbf{g}_2} A_{\mathbf{k}+\mathbf{g}_1} + \\ &+ 2 \sum_{\mathbf{g}_1} (\mathbf{k}+\mathbf{g}_1)_x (\mathbf{k}+\mathbf{g}_1)_y (\mathbf{k}+\mathbf{g}_3)_x (\mathbf{k}+\mathbf{g}_3)_y [\gamma]_{\mathbf{g}_2} A_{\mathbf{k}+\mathbf{g}_1} + \\ &+ \sum_{\mathbf{g}_1} (\mathbf{k}+\mathbf{g}_1)_y^2 (\mathbf{k}+\mathbf{g}_3)_y^2 [D]_{G_2} A_{\mathbf{k}+\mathbf{g}_1} + \\ &+ \sum_{\mathbf{g}_1} (\mathbf{k}+\mathbf{g}_1)_x^2 (\mathbf{k}+\mathbf{g}_3)_y^2 [\beta]_{\mathbf{g}_2} A_{\mathbf{k}+\mathbf{g}_1}, \end{aligned} \tag{8}$$

$\mathbf{g}_3 = \mathbf{g}_1 + \mathbf{g}_2$. Therefore, rewriting the Eq. (8) in matrix form:

$$\omega^2 \mathbf{P} A_{k+g_1} = \mathbf{Q} A_{k+g_1}. \tag{9}$$

Solving the Eq. (9), eigenfrequency is found, ω, for each real value of Bloch vector $\mathbf{k}$ within FIBZ (Vasseur, 1994).

1.2 Sierpinski Carpet

The squared unit cell center (size a) is the coordinate origin, Fig. 2. The number of grids for the L-stage is $N = M^{2L}$, where M is the initial grid number of the 1st-stage, and K is the number of gray sub-squares in the x or y direction. For the gray sub-squares in the central scatter, the central position of each sub-square can be defined as $\mathbf{r}_i = r_b + \frac{a}{M^L}(s-1)$, $s = 1, ..., KM^{L-1}$, where $i = x, y$; $r_b = a(1 - KM^{L-1})/2M^L$ represents the initial position of the first scale. Figure 2 shows the scheme example for distribution and positioning of fractals from the second stage.

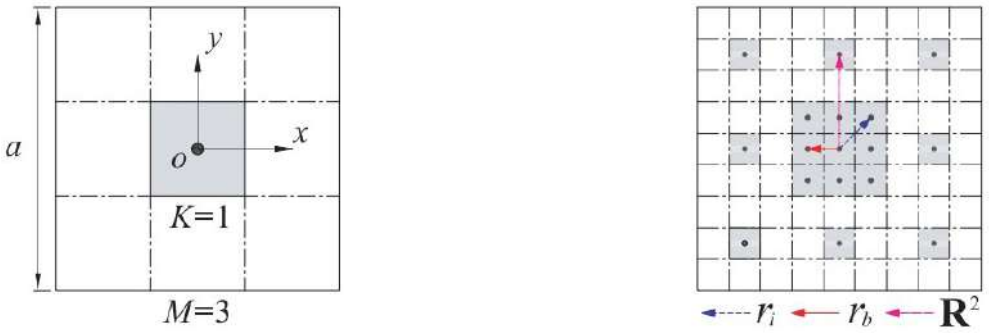

(a) (b)

Figure 2 – Distribution and positioning of fractals from the first (a) and second stage (b). Reprinted [adapted] from Huang et al. (2017)

.

1.3 Local Resonance

The base of PnC is the same, consisting of an epoxy matrix and the steel cylindrical inclusion, Fig. 3 (a). However, in the case of the implementation of local resonance, it will be formed by two coaxial cylinders. Thus, the PnC modeling is given from a heavy steel core (black), coated with a silicone ring (blue), both embedded in an epoxy resin matrix (gray). The inclusions are distributed in a square crystal lattice. The filling ratio is fixed and the work is carried out verifying the influence of the distribution of these LRs in Sierpinski fractals on the creation of gaps.

The physical parameters of epoxy, silicone and steel are listed in Tab. 1. The arrangement of the materials in the unit cell is given as follows:

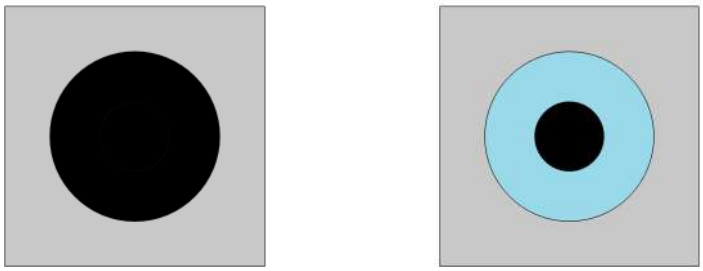

(a) (b)

Figure 3 – Unit cell with uncoated core - two materials (a) and coated - three materials (b).

Table 1 – Material properties (Shackelford, J.F. and Alexander, W., 2001)

Color	Material	Density [kg/m^3]	Young's Modulus [GPa]
Gray	Epoxy	2,500	40
Blue	Silicone	1,300	1.175
Black	Steel	7,875	210

2 SIMULATED RESULTS

The proposed method has been validated and shown to be accurate when comparing numerical results (FE/COMSOL) with analytical results (PWE). This is shown in Fig. 4, which shows the dispersion curves for the case of Fig. 3 (a). This case is considered a first stage quasi-Sierpinski fractal. It can be seen that there is a complete band gap and the wave propagation modes are represented by the color palette of the band structure. In the initial analysis, the PWE method was implemented only for a first-stage quasi-Sierpinski fractal, and will be implemented in the future for stages 2 and 3 of the fractal.

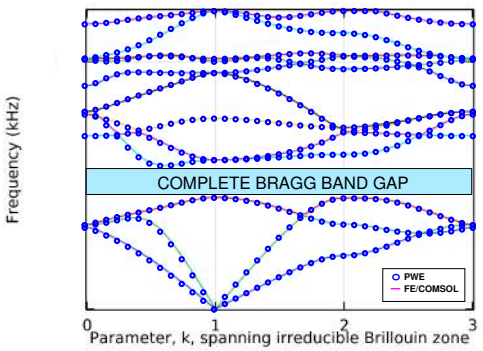

Figure 4 – Comparison of PnC results calculated by FE/COMSOL and by PWE

.

Extending the amount of wave modes presented by the PnC simulation, with the application of the first stage Sierpinski carpet fractal theory. The results via FE are shown in Fig. 5, where the z-directional wave mode forms in the third band (solid red line in Fig. 5) (b). In this case, where there is no local resonator, that is, it is a complete band gap of the Bragg, which ranges from 68 to approximately 80 kHz. We can observe through the wave mode (Fig. 5) (c), that the structure presents greater deformations in its central region, and that despite the impedance difference between the host material and the inclusion, there is a behavior of uniqueness of response.

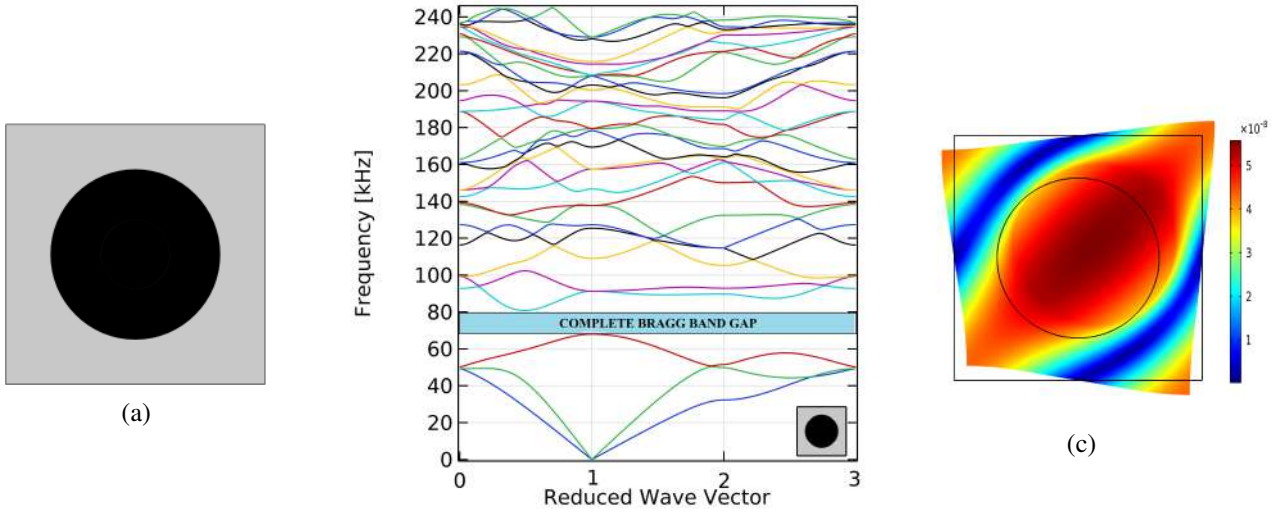

(a) (b) (c)

Figure 5 – (a) - Unit cell from first stage Sierpinski carpet fractal; (b) - PnC band diagram; (c) - wave mode shape at k = 1 and frequency of 68 kHz.

By creating the local resonance effect by introducing the steel core into a silicon ring, with the axial alignment, we determined very low frequency resonant modes, when compared to the case in the first stage fractal PnC. According to Yip and John (2021), this is due to the high density of modes, bringing extra and localized absorption. In Fig. 6 (b), the presence of propagating modes is observed in a small frequency bandwidth (up to 1440 Hz). In this interval, it is possible to verify in addition to the "sink" of the modes around the region Γ of the FIBZ (i.e., k=1). Moreover, two small complete Bragg band gaps are opened up.

For phononic crystals with the distribution of fractals in their second stage with the application of local resonance inclusions (Fig. 7), it is possible to clearly verify the behavior of the resonators in the wave mode shapes, since filtering by the resonance frequencies we have two intervals of movement: set to 258,92 and 373,69 Hz.

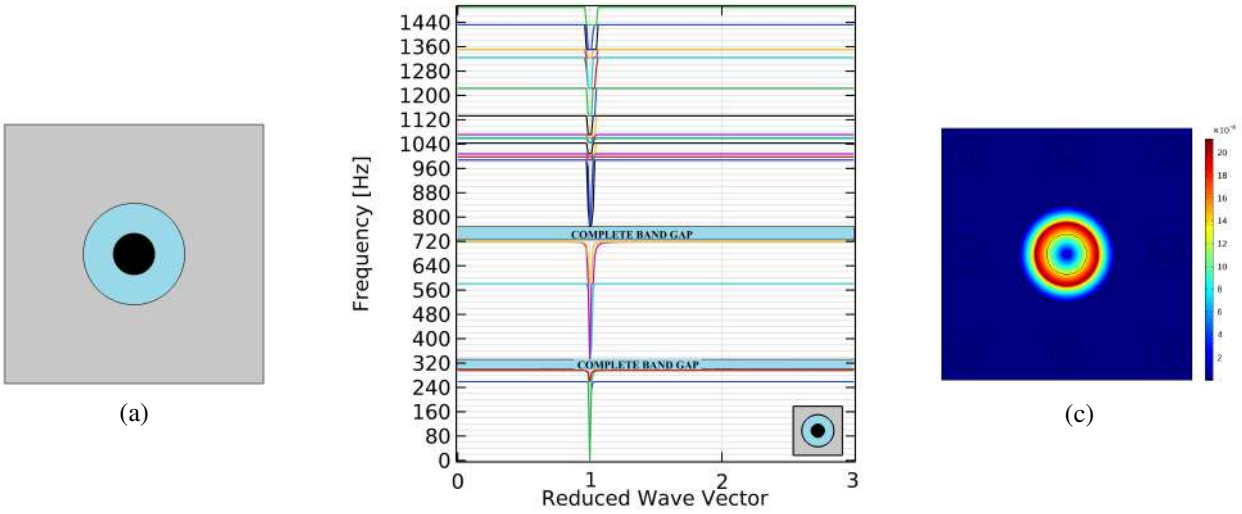

Figure 6 – (a) - Unit cell with local resonance - with three materials; (b) - band diagram with local resonance in a unit cell phononic crystal in k=1, resonant frequency: 258.92 Hz; (c) - wave mode shape shows the resonant mode at frequency of 258.92 Hz.

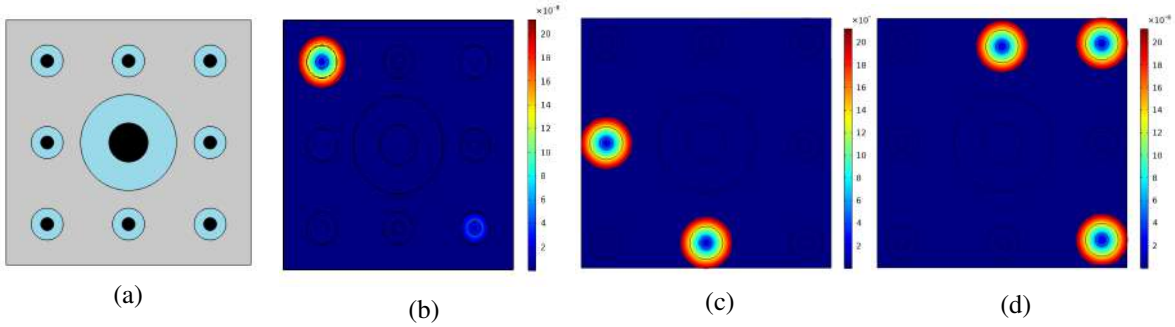

Figure 7 – (a) - Supercell model with fractal distribution - three materials; (b) - wave mode of only the resonant frequency of the central inclusion, set to 258,92 Hz; wave mode of fractal distribution inclusion's, set to 373,69 Hz for k=1.

3 FINAL REMARKS

In this work, we developed the theory of thin plates with the objective of evaluating the band structure in a PnC with steel inclusions in an epoxy matrix and its variations, as elements that cause local resonance, which were introduced in the configuration of a fractal PnC of Sierpinski-carpet. In addition to the case of the same PnC, but with the addition of mechanisms to enable the phenomenon of local resonance (LRPnC). Initially, we were successful in determining the band structure by the PWE method for the case of a first stage Sierpinski PnC carpet fractal, as well as a good convergence with the results found by the FE/COMSOL (Fig. 4). From Fig. 5, the presence of a complete Bragg band gap is observed around the 68 to 80 kHz bandwidth. It is verified that in this configuration there are no wave modes in very low frequency regions. On the other hand, for the LRPnCs it was observed (Fig. 6), the local resonance that was provoked with the addition of a silicon ring element that surrounds the steel core in the epoxy resin matrix, guarantees the presence of localized modes of low frequency and flat bands, showing small "sags" in the modes that appear in the band structure. Another point is the observation of narrow and full band gaps locally resonant at low frequencies is the visualization of wave modes. We observed that with the increase of the fractal stage, the second stage has the potential to manipulate the propagation of the sound wave to specific frequencies, since the structure is perceived by concentrating the vibration in the resonant frequencies of the inclusions. We estimate that our simulated study provides motivations for research into applications involving phononic crystals and new cell geometries and how this influences band structures and wave modes.

ACKNOWLEDGMENTS

The authors gratefully acknowledge the support of the Brazilian funding agencies CAPES (Finance Code 001), CNPq (Grant Reference Numbers 317436/2021, 151311/2020-0 and 403234/2021-2), FAPEMA (Grant Reference Numbers 002558/21, 02559/21 and 00680/22), FAPESP (Grant Reference Number 2018/15894-0) and IFMA.

REFERENCES

Arjunan, A., Baroutaji, A., and Robinson, J., 2022, "Advances in Acoustic Metamaterials", Encyclopedia of Smart Materials, Elsevier, pp; 1-10, ISBN 9780128157336

Goffaux, C., Sánchez-Dehesa, J. and Levy Yeyati, A., 2002, "Evidence of Fano-Like Interference Phenomena in Locally Resonant Materials", Physical Review Letters, Volume 88, Number 22

Gupta, A., 2014, "A Review on Sonic Crystal, Its Applications and Numerical Analysis Techniques", Acoustical Physics, Volume 60, pp. 223-234.

Huang, J., Shi, Z. and Huang, W., 2017, "Multiple band gaps of phononic crystals with quasi-Sierpinski carpet unit cells", Physica B, Volume 516, pp 48-54.

Huang, J., Ruzzene, M. and Chen, S., 2017, "Analysis of in-plane wave propagation in periodic structures with Sierpinski carpet unit cells", Journal of Sound and Vibration, Volume 395, pp.127-141.

Khouloud, S., Ketata, H. and Ben Ghozlen, M., 2019. "Locally resonant phononic crystals band-gap analysis on a two dimensional phononic crystal with a square and a triangular lattice", Optical and Quantum Electronics. 51.

Kuo, N.K. and Piazza, G., 2011. "Fractal phononic crystals in aluminum nitride: An approach to ultra high frequency bandgaps", Applied Physics Letters, Vol. 99.

Miranda Jr., E.J.P., Angelin, A.F., Silva, F.M., and Dos Santos, J.M.C., 2019, "Passive vibration control using a meta-concrete thin plate", Cerâmica 65 (2019) Suppl.1 27-33.

Sigalas, M.M., Economou, E.N., 1992, "Elastic and acoustic wave band structure", Journal of Sound and Vibration, Volume 158, Issue 2, pp 377-382, ISSN 0022-460X.

Spiousas, I., Etchemendy, P.E., Vergara, R.O., Calcagno, E.R., and Eguia, M.C., 2015, "An Auditory Illusion of Proximity of the Source Induced by Sonic Crystals', PLOS ONE 10(7).

Shackelford, J.F. and Alexander, W., 2001, "Materials Science and Enginnering Handbook", CRC Press LLC, 3th edition.

Vasseur, J.O., Djafari-Rouhani, B., Dobrzynski, L., Kushwaha, M.S. and Halevi, P., 1994, "Complete acoustic band gaps in periodic fibre reinforced composite materials: the carbon/epoxy composite and some metallic systems". Journal of Physics: Condensed Matter, Vol. 6, No. 42, pp. 8759–8770.

Yip, K.L.S. and John, S., 2021, "Acoustic modes of locally resonant phononic crystals: Comparison with frequency-dependent mass models", Phys. Rev. B, American Physical Society, Vol. 103.

RESPONSIBILITY NOTICE

The authors are the only parties responsible for the printed material included in this paper.